Global warming induced hybrid rainy seasons in the Sahel

2016 Environ. Res. Lett. 11 104008

(http://iopscience.iop.org/1748-9326/11/10/104008)

Environmental Research Letters

LETTER

Global warming induced hybrid rainy seasons in the Sahel

Seyni Salack[1,2], **Cornelia Klein**[1,3], **Alessandra Giannini**[4], **Benoit Sarr**[5], **Omonlola N Worou**[2], **Nouhoun Belko**[6], **Jan Bliefernicht**[3] **and Harald Kunstman**[1,3]

[1] Institute of Meteorology and Climate Research, Atmospheric Environmental Research (IMK-IFU), Karlsruhe Institute of Technology (KIT), Kreuzeckbahnstr. 19, D-82467 Garmisch-Partenkirchen, Germany
[2] WASCAL Competence Center, West African Science Service Center on Climate Change and Adapted Land Use (WASCAL CoC), 06 BP: 9507 Ouagadougou, Burkina Faso
[3] Institute of Geography, Chair for Regional Climate and Hydrology, University of Augsburg, D-86135 Augsburg, Germany
[4] International Research Institute for Climate and Society, The Earth Institute, Columbia University, PO Box 1000, Palisades, NY 10964-8000, USA
[5] Département Formation et Recherche (DFR), Centre Régional AGRHYMET (CRA), BP 11011, 425 Boulevard de l'Université, Niamey, Niger
[6] International Institute of Tropical Agriculture (IITA), Kano Research station, Sabo Bakin Zuwo Road, PMB 3112, Kano, Nigeria

E-mail: seyni.salack@kit.edu **and** salack.s@wascal.org

Keywords: hybrid season, drought thresholds, agroclimatic monitoring, Sahel, global warming

Supplementary material for this article is available online

OPEN ACCESS

RECEIVED
24 December 2015

REVISED
22 July 2016

ACCEPTED FOR PUBLICATION
29 July 2016

PUBLISHED
5 October 2016

Abstract

The small rainfall recovery observed over the Sahel, concomitant with a regional climate warming, conceals some drought features that exacerbate food security. The new rainfall features include false start and early cessation of rainy seasons, increased frequency of intense daily rainfall, increasing number of hot nights and warm days and a decreasing trend in diurnal temperature range. Here, we explain these mixed dry/wet seasonal rainfall features which are called hybrid rainy seasons by delving into observed data consensus on the reduction in rainfall amount, its spatial coverage, timing and erratic distribution of events, and other atmospheric variables crucial in agro-climatic monitoring and seasonal forecasting. Further composite investigations of seasonal droughts, oceans warming and the regional atmospheric circulation nexus reveal that the low-to-mid-level atmospheric winds pattern, often stationary relative to either strong or neutral El-Niño-Southern-Oscillations drought patterns, associates to basin warmings in the North Atlantic and the Mediterranean Sea to trigger hybrid rainy seasons in the Sahel. More challenging to rain-fed farming systems, our results suggest that these new rainfall conditions will most likely be sustained by global warming, reshaping thereby our understanding of food insecurity in this region.

1. Introduction

According to recent global warming perspectives, increased heating may not cause droughts but it is expected that when droughts occur they are likely to set in quicker and be more intense [1]. What if the often discussed recovery of Sahel rainfall [2–5, 7] is attributable to an increased frequency of intense rain events while the spatio—temporal distribution is similar to drought conditions? Such *hybrid*—mixed dry and wet features–rainy conditions would be more challenging to food security. Even if seasonal average rainfall amounts are recovering from the previous drought years, the distribution of rain events and associated maximum and minimum temperature extremes [8] determine the success or failure of local smallholder farming systems.

However, the use of areal agro-meteorological monitoring metrics does not depict these potential risk factors. On the one hand, the *adhoc* drought monitoring metrics, based on rainfall and other variables, are proven sensitive to mathematical formulations and the baseline period used to establish the reference climatology [1, 2]. On the other hand, seamless predictions are hampered by large uncertainties resulting from limited information concerning the future of El-Niño Southern-Oscillations (ENSO) [1], the possible combined effects of oceans warming [5, 9],

anthropogenic aerosols and atmospheric greenhouse-gases (GHGs) forcing on the natural variability of rainfall [10, 11]. The need arises to investigate new standards for agroclimatic drought (flood) monitoring, and provide regional perspectives for predictions.

In the Sahel, adequate monitoring metrics need to include rainfall timing (i.e., principal season of occurrence, delays in the start of the rainy season, occurrence of rains in relation to sensitive crop growth stages), the distribution of rain events (i.e. rainfall intensity, number of rainfall events) and the spatial coverage [12–14]. Other factors such as high diurnal temperature ranges, high wind speeds, low relative humidity, high evapotranspiration and soil moisture depletion, often associated with drought conditions, may increase the severity of the event. In this paper, we define a new basis for drought identification by reconciling observational datasets. We further investigate how both oceans basin warming and the regional dynamic features in the low-to-mid level atmosphere are involved in triggering droughts and hybrid rainy seasons. These hybrid rainy seasons are considered as a new threat to rain-fed farming systems that calls on the use of novel climate information services for food security in the region.

2. Data and methods

2.1. Data sets

2.1.1. In situ and gridded data

The Sahel is defined here as the sub-Saharan region that stretches from the western coasts of Senegal in West Africa to the North-Eastern edges of the Sudan and Ethiopia in East Africa between 10 to 20°N. The rainy season of this region is dominated by the West African monsoon which is confined between May to October with June–September explaining the most important amount of the seasonal totals. Observed station data (In-situ data), including daily rainfall, maximum and minimum temperature and other variables, were contributed by the meteorological services and agencies of the West African countries to www.wascal.org and www.agrhymet.ne following specific data sharing policies. In this assessment, 112 rainfall recording stations have quality controlled daily time series from 1950 to 2010. Among these 112 stations, there are 65 primary synoptic stations that provide also daily minimum and maximum temperatures from 1960 to 2012. They are well spread across 10–20°N and 16°W–20°E and the majority fall within the region where average annual rainfall is between 200 mm to little less than 1100 mm (supplementary figure 1). All historical data sets of rainfall and temperatures are used to compute some agroclimatic indices. This *in situ* data is reconciled with three other open source gridded data sets to extract the cluster of spatially coherent, synchronous and persistently dry seasons irrespective of baseline climatology (see methods).

Monthly precipitation data sets of NOAA's Precipitation Reconstruction over Land (CPC-P/L), CRU.TS3.21, and GPCC v6 are processed on a regular 0.5° × 0.5° grid based on world-wide station records. CRU.TS3.21 daily temperature range (DTR) data are also used. CRU.TS3.21 data are available from http://badc.nerc.ac.uk/browse/badc/cru/data/cru_ts/cru_ts_3.21/data. The gridded data has longer time series than the *in situ* data set. We extracted only the longest common time series to all data sets (i.e. 1960–2010) for the consensus analyses (figure 1). Monthly Extended Reconstructed Sea Surface Temperature (ERSSTv4) dataset is available on global 2° × 2° grids, surface pressure and U-V wind components are taken from NCEP/NCAR Reanalysis 1 on a 2.5° × 2.5° grids, model-calculated soil moisture depth (CPC Soil moisture) is on a 0.5° × 0.5° grid and NOAA's top of atmosphere Outgoing Longwave Radiation (OLR) dataset comes from a 1° × 1° grid (1979–2012). CPC-P/L, GPCC, CPC soil moisture, ERSSTv4 and NCEP/NCAR Reanalysis 1 data sets are provided by the NOAA/OAR/ESRL PSD, Boulder, Colorado, USA, from their Web site at http://www.esrl.noaa.gov/psd/.

2.2. Methods

2.2.1. Agroclimatic monitoring indices

The seasonal and intra-seasonal agro-climatic indices are defined based on the combination of *in situ data*, gridded data and crop model simulations (supplementary tables 1 and 2). From the daily *in situ* data, we define the date of the first efficient rainfall as the day after May 1 when 20 mm totaled over 1 to 3 days is not followed by a dry spell ⩾20 days in the next 30 days. The cessation date is the day after September 1 when soil water content is ⩽0.05 mm mm^{-1} [6, 13]. The soil water content criterion is based on a simple water balance model for which the average potential soil evaporation per day is taken as 5 mm d^{-1} and storage limit as 100 mm. For the crop simulations, we used the *Decision Support System for Agrotechnological Transfer* version 6 (DSSATv4.6) cropping system model [32], calibrated and tested for some millet, maize and cowpea cultivars. It was calibrated for pearl millet cultivars (HKP, Souna 3, Zatib), cowpea cultivars (IT98k-205-8 and IT98K-503-1) using experimental data collected at AGRHYMET (Niamey) in 2002–2003 (detailed descriptions of the experiments are provided in Salack *et al* [6]), at Bambey station (Senegal) in 1996–1997 and 2008–2009 for cowpea (detailed descriptions of experiments are found in Belko *et al* [16]). The CERES and CROPGRO modules of DSSATv4.6 are calibrated and tested using both on-farm surveys and field trials conducted at and around experimental stations of Bambey (Senegal), Kano (Nigeria), Niamey (Niger) and Sarria (Burkina Faso).

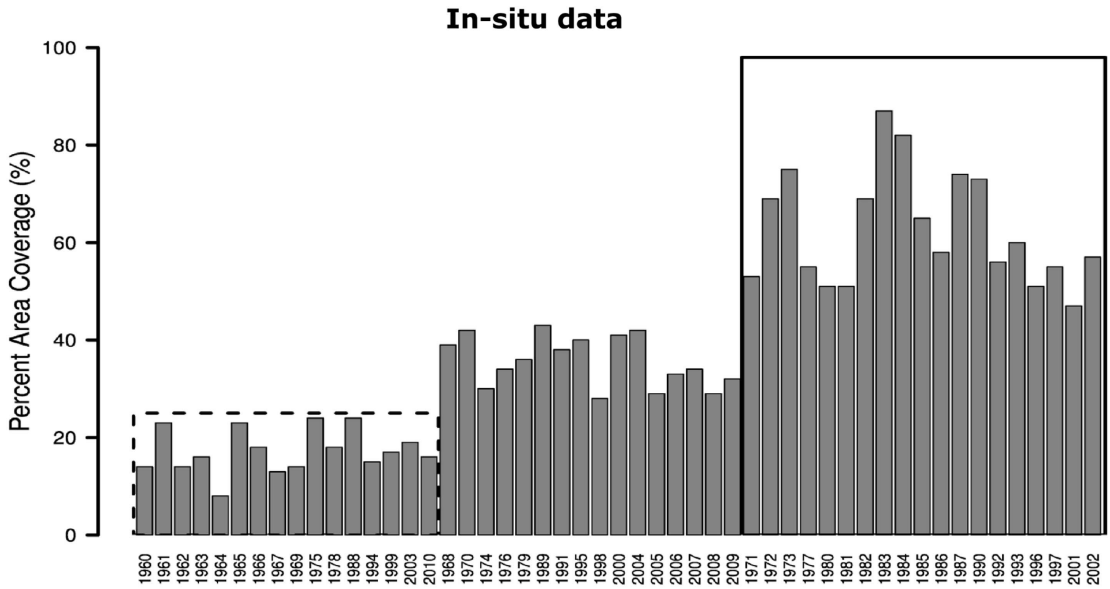

	Wet cluster (WtC)	Drought cluster (DtC)
CRU-TS3.21	1960, 1961, 1962, 1963, 1964, 1965, 1966, 1967, 1969, 1975, 1978, 1988, 1994, 1998, 1999, 2003, 2005 2010	1971, 1972, 1973, 1982, 1983, 1984, 1985, 1986, 1987, 1989, 1990, 1992, 1993, 1996, 1997, 2001, 2002
CPC-Prec/L	1960, 1961, 1962, 1963, 1964, 1965, 1966, 1967, 1975, 1978, 1988, 1994, 1998, 1999, 2003, 2005, 2008, 2010	1971, 1972, 1973, 1977, 1982, 1983, 1984, 1985, 1986, 1987, 1990, 1992, 1997, 2000, 2001, 2002, 2004
GPCC v6	1960, 1961, 1962, 1963, 1964, 1966, 1967, 1969, 1974, 1975, 1978, 1988, 1994, 1998, 1999, 2003, 2008, 2010	1971, 1972, 1973, 1982, 1983, 1984, 1985, 1986, 1987, 1990, 1992, 1993, 2000, 2001, 2002, 2004
Consensus	1960, 1961, 1962, 1963, 1964, 1966, 1967, 1969, 1975, 1978, 1994, 1998, 1999, 2003, 2008, 2010	1971, 1972, 1973, 1982, 1983, 1984, 1985, 1986, 1987, 1990, 1992, 1993, 2001, 2002

Figure 1. Classification of dry/wet seasons from different data sets. The clusters of dry seasons with area coverage from the *in situ* data and gridded data sets CRU-TS3.21, CPC-Prec/L and GPCC v6. The consensus years of strong and very strong El-Niño (La-Niña) years [15] are underlined.

The sensitivity tests simulations are described in supplementary note 2. Using DSSATv4.6 [32], we define the planting date as the first day between April 1 and July 31 when at least 40% soil moisture in the top 20 cm depth is reached, daily minimum temperature does not drop below 11 °C for millet and cowpea cultivars (below 8 °C for maize) and maximum temperature does not exceed 35 °C [6]. Post-floral dry spells are consecutive dry days observed fifty days after planting date. For agronomic reasons a dry day is defined as the day when cumulated rainfall is <1 mm d^{-1} [13] and intense rainfall is the 95th percentile of the 6 month block daily rainfall.

2.2.2. Areal classification of dry seasons

Due to differences in data assimilation methods, interpolation techniques and the number of stations involved, rainfall information provided by gridded data sets of different global data centers vary significantly [1, 17] (supplementary figure 2). To work around this discrepancy, spatially coherent, synchronous and persistently dry seasons are extracted from the consensus of both meteorological station data (*in situ* data, 1960–2010) and the aforementioned gridded data sets (1960–2012) for the Sahel region. Our main hypothesis is that the rainy season at each station can have a spatially uniform component shared simultaneously with several other stations in the region. We write the individual j station (grid point) time series of the seasonal agro-climatic indices as I_{ij}^{b} where i denotes the year ($i = 1\ldots N$), and $b = \{1960–2010, 1961–1990, 1971–2000, 1981–2010, 1991–2010\}$ denotes the *baseline period*

$$I_{ij}^{b} = \begin{cases} 1, & \text{if } \lambda_{ij}^{b} < 0, \\ 0, & \text{otherwise.} \end{cases} \quad (1)$$

where

$$\lambda_{ij}^{b} = \frac{x_{ij} - \overline{x_{jb}}}{\sigma_{jb}},$$

with λ_{ij}^{b} as the zero mean and unit variance anomaly, $\overline{x_{jb}}$ and σ_{jb} are the mean and inter-annual standard deviation for baseline b at station j, ($j = 1\ldots M$). The sampling of the baseline takes into account the sensitivity of the anomaly to baseline climatology shown by Trenberth *et al* [1]. It enables composite

group of dry (wet) seasons to be formed based on the most persistently negative (positive) trend of the index, irrespective of baseline climatology. This baseline sampling embeds the long term trends and variability found in historical rainfall assessments over this region namely wet, dry and recovery [2, 3, 6]. In the case of the 6 month (May–October) seasonal rainfall amount, we choose the threshold −0.25 as the number of standard deviations from the mean at which a year is considered abnormally dry over the region in order to approximately match the intensity of abnormally dry years in the case of other monitoring indices [18, 19] and ensure a minimum spatial coherence of identified dry spells [14]. The spatial extent (SE) of a drought event is measured from the anomaly index synchronous over M stations:

$$\mathrm{SE}_i = 100 * \left(\frac{1}{B}\sum_{b=1}^{B} E_i^b\right), \qquad (2)$$

where $E_i^b = \frac{1}{M}\sum_{j=1}^{M} I_{ij}^{\,b}$.

For every baseline period b, SE_i indicates the seasonal area coverage of synchronized drought over the region. All SE time series are clustered using an agglomerative hierarchical clustering technic based on pairwise Euclidean distance between individual baseline values. The number of classes is chosen, from the dendrogram of classes, at the maximum branching gap below which the interclass differences are statistically significant at the 5% level according to a '*pooled variance*' two-tailed t test. Three clusters of rainy seasons are hereby identified. The drought cluster (DtC) is composed of years with a precipitation deficit of at least −0.25 standard deviation and at least 50% area coverage (figure 1). The seasons with a precipitation deficit of at least −0.25 standard deviation and an area coverage less than 25% are considered 'locally dry' but with a regional scale wet index. They form the wet cluster (WtC). We define a consensus amongst the observational data sets when a season is found dry (wet) in all data sets. Years which do not fall within the DtC (WtC) category are considered intermediate (INT). The sensitivity of the SE_i index was tested over the entire region, by sampling country-by-country catchment (to test the sensitivity of change in number of stations per sample) , and by gridding the *in situ* data on regular 0.5° × 0.5°, 1° × 1° and 2° × 2° grids respectively.

For further analyses, we also consider SST anomalies (SSTAs) for the Niño 3.4 region (5°N–5°S, 120–170°W). We computed the November–December–January running average SSTAs taken from ERSST v4 for which El-Niño (La-Niña) are defined according to the thresholds given by NOAA-Climate Prediction Center [15]: weak El-Niño (La-Niña) when the anomalies fall between 0.5° and 0.9° (−0.5° and −0.9°), moderate between 1.0° and 1.4° (−1.0 and −1.4 anomaly), strong between 1.5 and 1.9 and very strong when the anomalies are ⩾2.0 (⩾−2.0). As found earlier, years in which the north Atlantic is warmer than the global tropical oceans the Sahel will receive abundant rains as a result of increased moisture supplied in monsoon flows [5, 9, 21]. Here, the new seasonal predictability index we are suggesting consists of subtracting the north Atlantic (10–75°N, 75°W–15°E) from the global SST before computing the anomalies by subtracting the average climatology from the time series. Other oceanic basins SSTAs analyzed during the June–September season include subtropical north Atlantic (sub_NATL, 10–40°N, 15–75° W), the extra-tropical north hemispheric Atlantic (NH_NATL, 30–75°N, 15–75°W), the Mediterranean sea (MEDIT, 0–35°E, 30–44°N), the equatorial Atlantic (Eq_ATL, 5 S–5°N, 40°W–15°E), the South Atlantic (SH_ATL, 10 s-0°N, 20°W-10°E) and the Eastern Equatorial Indian ocean (Eq_IND, 15°S–15°N, 50–90°E) (figures 3(c)–(d) and supplementary figure 5).

3. Results

3.1. Seasonal droughts, SST warming and regional atmospheric circulation nexus

The rainy seasons of the DtC are characterized by higher rainfall deficit with larger spatial variance which is also visible in the seasonal cycles (supplementary figure 3), including late onset and shorter durations of the cropping season (figure 2). Long dry spells after planting and during the flowering phase of rain-fed crops are the key hazards that determine the failure of rain-fed farming systems [6, 13, 14]. The soil moisture deficits added to low soil fertility, high temperatures and evaporation rates increase the rate of agroclimatic risks inherent to seasonal droughts. Further analyses reveal also a significant inverse co-variability of DTR, rainy days and rainfall amount which is enhanced during extreme droughts (supplementary figures 4(a)–(b)). All over the Sahel, dry seasons exhibit larger amplitude of DTR anomalies compared to wet years as a result of seasonal fluctuations in moisture fluxes and radiative heating (supplementary figures 4(c)–(d)). The strong relationship between DTR, rainy days and rainfall amount makes DTR anomalies useful to detect drought flags such as intra-seasonal spells, the subseasonal heat stress and can also determine onset/cessation of cropping season in the Sahel. Table 1 summarizes the threshold values which combination, during the life cycle of staple field crops, strains their growth, development and production, if optimum crop management measures are not applied by the farmer. These average values are estimated from the seasons of the DtC and constitute the critical limits for most cropping systems to be sustained over larger portions of the Sahel region. We also believe that any environmental variable drawn from the DtC cluster

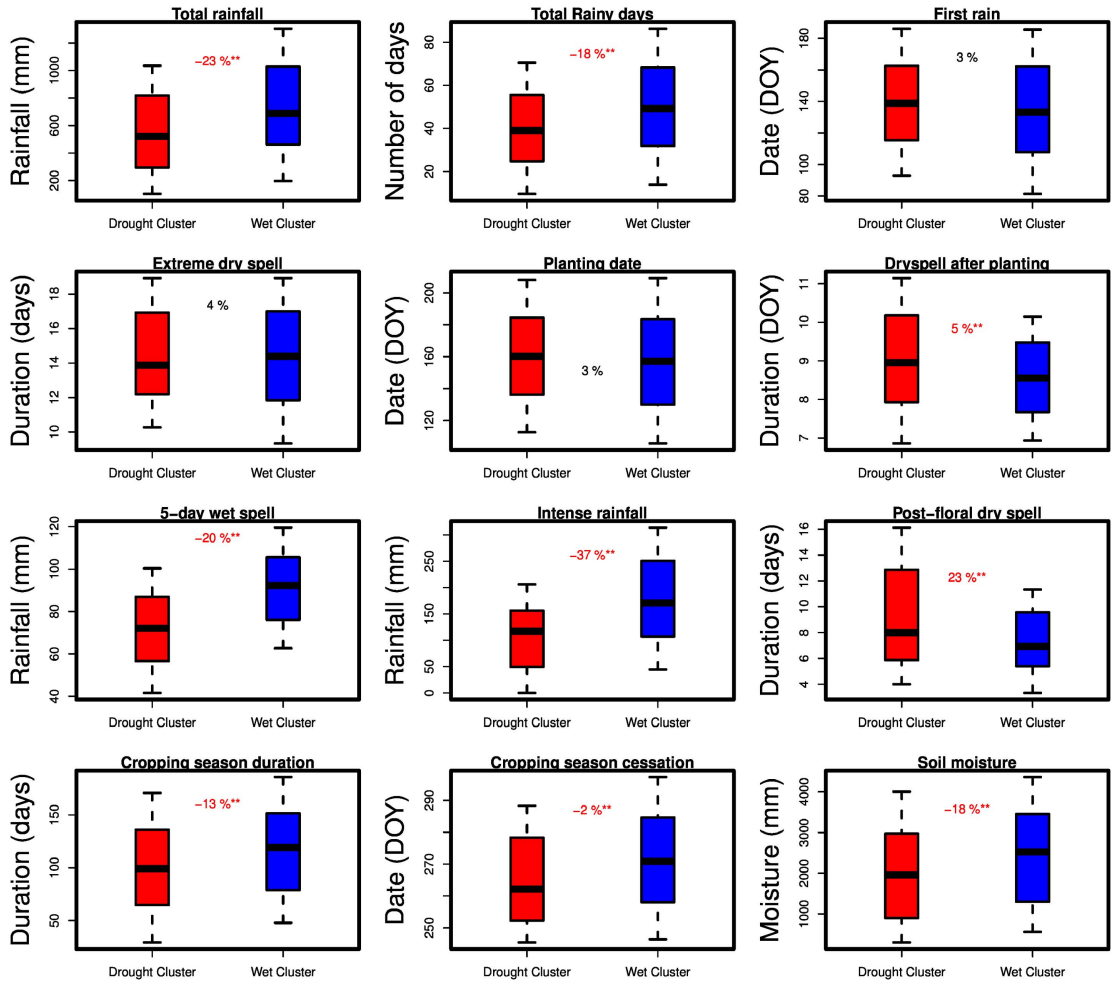

Figure 2. Agro-climatic indices comparison between drought and wet clusters. The percent difference is given by the number between boxes (**) is statistically significant at 95% confidence level according to a *pulled-variance* Student *t-test*. The boxes and whiskers denote the spatial distribution across the Sahel. The horizontal segment inside boxes: median and whiskers: minimum/maximum.

Table 1. Threshold values characterizing seasonal droughts in the Sahel and their percent difference with 1991–2013 time series. The parameters $\overline{\lambda}$ and σ_{sp} are the area average and spatial distribution offset (standard deviation). The positive (negative) sign is an increase (decrease).

	Drought cluster		1991–2012		Difference
Index	$\overline{\lambda}$	σ_{sp}	$\overline{\lambda}$	σ_{sp}	(%)
Total rainfall (mm)	569.8	299.4	721.4	48.8	+21[a]
Number of Rainy days (#)	42	22.5	47.3	3.1	+12[a]
Date of first rain event (DOY)	138	35d.	133	34d.	−3
Extreme dry spell (days)	18	16	9	1	−109[a]
Planting date (DOY)	154	44d.	151	15.6	−1
Dry spell after onset (days)	9	2	8.6	1	−1
5-day wet spell (mm)	73.7	22.1	91.2	8.8	+19[a]
Intense rainfall (mm)	108.9	66.7	154.9	86.5	+30[a]
Post-floral dry spell (days)	10	6	9	1	−17[a]
Cropping duration (days)	102	44	116	6	+12[a]
Cropping cessation date (DOY)	244	13d.	245	14d.	+1
Soil moisture (mm)	165.8	94.3	276.3	21.6	+40[a]
Daily temperature range (°C)	10	1.9	10	1.3	−1

[a] Statistically significant at 95% confidence level using a pulled-variance *Student t-test*. ** *d.* = day(s).

can be considered as reference baseline threshold useful in monitoring and early warning under climate change.

The Sahel is a remote ENSO-sensitive tropical region and usually, droughts cover more than twice the land area in years of a strong versus weak El-Niño

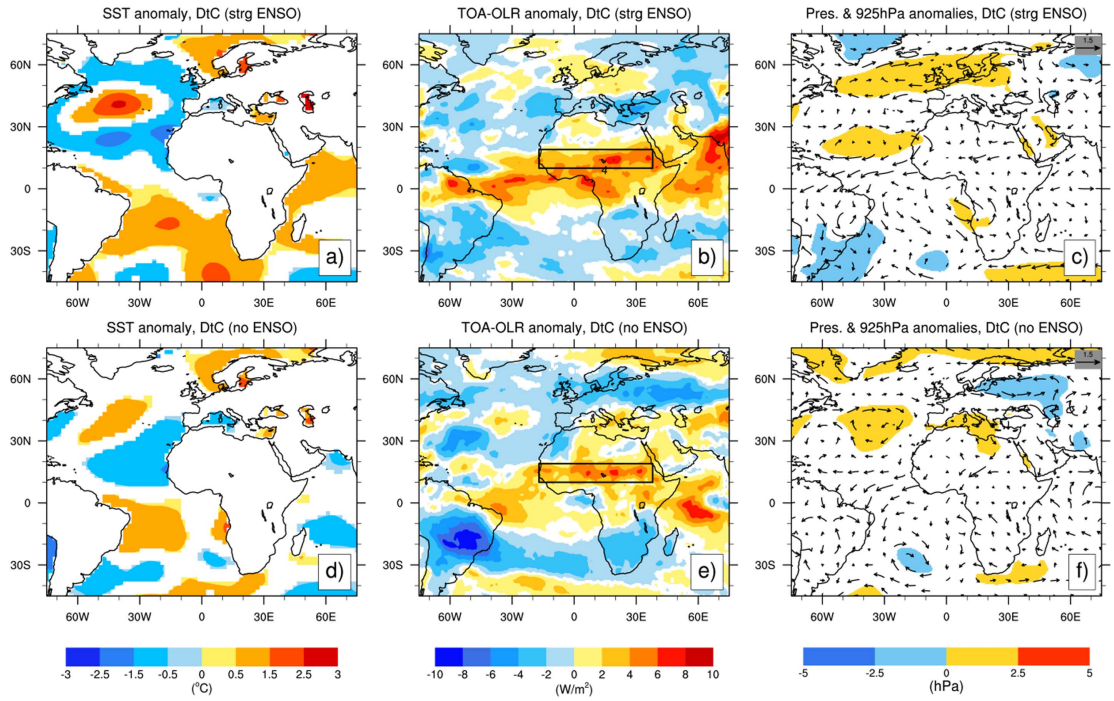

Figure 3. Average June–September anomalies and atmospheric wind profile in drought clusters (DtC) of strong/very strong ENSO (strg ENSO), weak/neutral ENSO years (no ENSO). Only statistically significant features are drawn. The black rectangle determines the Sahel. Factors in (a)–(f) include Sea Surface temperature anomaly (SSTA), Top-of-atmosphere-Out-going Longwave Radiation anomaly (OLRA), Surface Pressure anomaly (Pres.) & 925 hPa wind anomaly. Westerly and southerly directions indicate positive anomalies. Only vectors for which at least one component is larger than 1.5 m s^{-1} are plotted. The u-wind anomalies in (g)–(j) are relative to 1981–2010 climatology. Above 700 hPa, positive (negative) u-wind anomalies represent weakened (strengthened) easterly wind.

event (warm ENSO) [19]. The rainy seasons in the Sahel are also affected by other regional scale atmospheric factors which may trigger dryness even when ENSO signal is weak or neutral (supplementary note 1). In dry years associated with strong/very strong November–December–January ENSO signal (strg ENSO, herewith), warm sea surface temperature anomalies (SSTAs) are found in the Equatorial eastern/central Pacific (Nino3, Nino3.4 regions) [15]. Spatially coherent droughts are regulated by stronger East-West Walker circulation cells forcing anomalous subsidence of dry air over the West and East African regions [20, 21]. The descending air weakens the Hadley cell by slowing down the near surface, low level southerly winds and reducing both moisture flux and the rate of deep convection over the region [22, 23] (figures 3(a)–(c)). Meanwhile, a wide spread continental radiative heating, resulting from less cloud cover, increases the diurnal temperature range (DTR) and reduces the meridional temperature gradient over the continent. This situation coincides with a dipole in the Atlantic Ocean with negative SSTAs north of 10°N, positive south and in the equatorial Indian Ocean. As the Sahel dries, the intensity of the Indian monsoon also reduces [20]. The weakening of the tropical divergent circulations (i.e. the Walker and local Hadley circulations) causes changes in energetic maintenance of the Tropical Easterly Jet (TEJ) [24, 25]. The African Easterly Jet (AEJ) becomes more enhanced and extended (figure 3(g)), suppressing convective activities in the Inter-tropical Convergence Zone (ITCZ). A weaker TEJ aligned with an enhanced AEJ, and a southward-shift of the ITCZ result in a reduced frequency of westward propagating mesoscale convective systems (MCS) [25]. These MCS contribute the majority of rainfall events in the Sahel [26]. Late onset and extreme dry spells are experienced in such dry seasons and the energy thresholds needed to supply moisture into the ITCZ and trigger deep convection are met late July [14].

When ENSO signal is weak or neutral (no ENSO, herewith), drought may occur as well. In this case, there is a shallow generalized warming of the tropical oceans and deep convection is observed over the Eastern Latine America which contributes to weaken the sub-tropical high pressure center at its northerly position in the south Atlantic (figures 3(d)–(f)). This reduces the strength of the penetrating cross-equatorial south-westerlies causing the shallow low-levels moisture inflow [22, 23]. In the North Atlantic, the sub-tropical basin becomes warmer than the extra-tropical North Atlantic basin (NH_NATL). The negative SSTAs in the NH_NATL and the Mediterranean Sea (MEDIT) are associated with positive surface pressure anomalies of the subtropical high pressure belt including its Libya-Egypt eastern extension. This creates a strong and consistent inflow of northeasterly winds over the Sahel preventing further migration of the

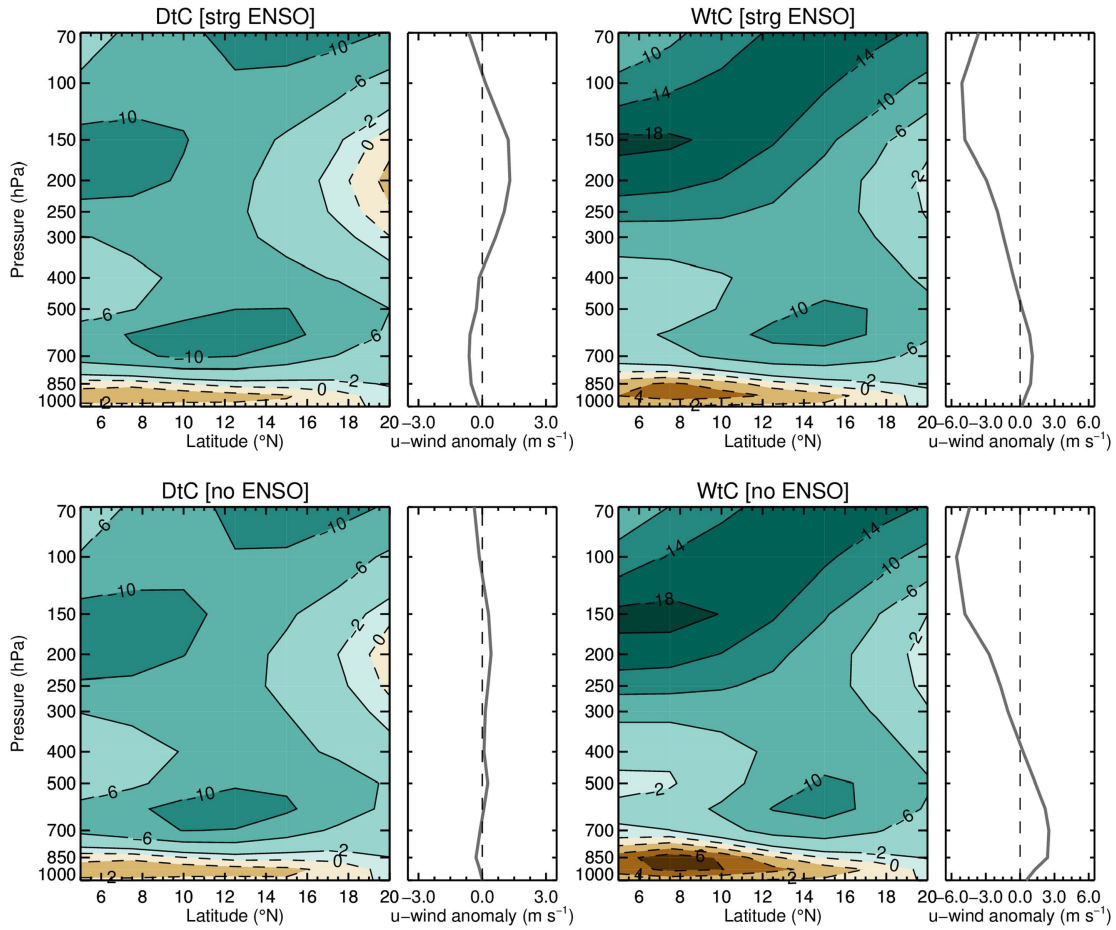

Figure 3. (Continued.)

rain-belt [22, 25]. These particular atmospheric patterns found in the seasons of the drought cluster (DtC) are reversed or absent in the wet cluster (WtC) (supplementary figures 5(a)–(f) and supplementary figure 6).

3.2. Explaining the post-1990 hybrid rainy seasons

From the consensus of all data sets, only five (six) seasons of the DtC (WtC) fall within the period post-1990 (including the year 1990) (figure 1). Ten dry seasons encountered in this assessment are categorized as intermediate (INT) with an area coverage in the interval]25%; 50%[. The comparative analysis of the 1991–2012 periods with DtC seasons shows a similarity of distribution of rainfall events even though a higher rainfall amount is recorded (table 1). This confirms that the rainfall distribution exhibits drought characteristics and the recovery of average rainfall amounts is explained by an increase of intense rainfall and wet spells [6, 7]. The spatial variability of these parameters is relatively homogenous over the region as opposed to DtC (table 1). In this mixed dry/wet sub-seasonal characteristics of rainy seasons, farm planning becomes difficult.

The ENSO signal in the seasons of the INT cluster is weak-to-moderate El-niño (except for 1997 which was classified as very strong El-niño year) [15]. The June-to-September regional low-to-mid level circulation patterns of the INT (post-1990) are stationary relative to those found in dry years of weak-to-neutral El-Niño signal (figures 4(a) and (b)). In contrast there is a top-to-bottom asymmetric wind speeds in the INT (pre-1990) in which the TEJ is strong coinciding with much warmer sub-tropical north Atlantic and south Atlantic (figures 4(c) and (d)). The warming of these basins has a combined positive effect of raising the thresholds for deep convection to occur by increasing moisture supply to the monsoon flow [5, 9, 21]. With the strong TEJ, the upper-level divergence is enhanced [24, 25], sustaining thereby a relatively strong Hadley cell circulation over the region that counter balances the large scale subsidence imposed by weak-to-moderate El-Nino [20]. However, in the post-1990 INT types of drought, the TEJ becomes weak. The AEJ is relatively enhanced with extended core and its vertical axis aligning with that of the TEJ like in the case of 1983 described by Nichoson [25]. Similarly to DtC (no ENSO) situations, shallow warming occurs in the north Atlantic but much in the MEDIT. A warmer MEDIT enhances moisture content in the lower troposphere that is advected southwards into the Sahel by the low-level mean flow across the eastern Sahara [27].

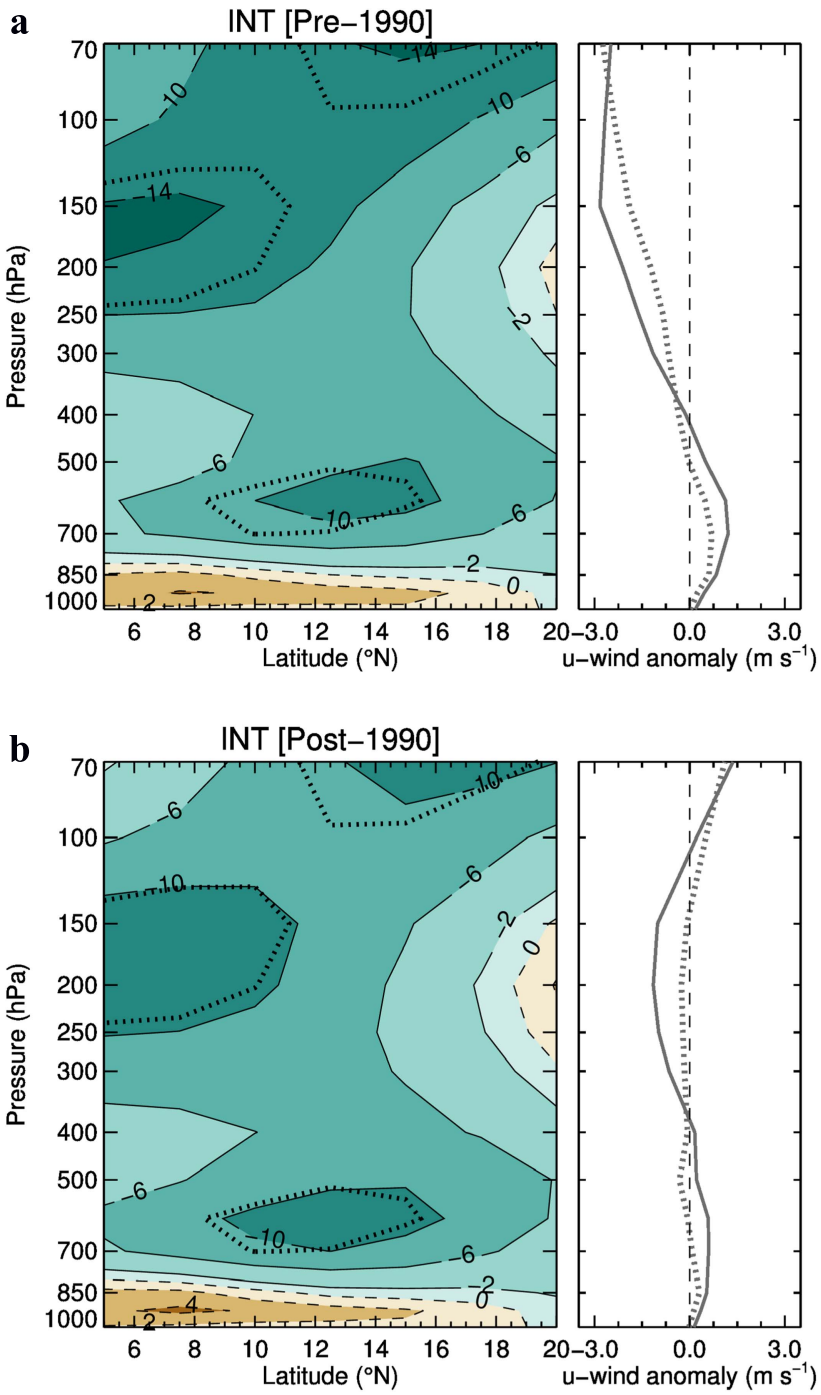

Figure 4. Average June–September atmospheric wind profiles and SSTAs in oceanic basins of INT drought cluster. Pre-1990 (1965, 1968, 1970, 1974, 1976–77, 1979, 1980–81, 1988–89) and Post-1990 (1991, 1995–97, 2000, 2004–05, 2004–07, 2009). The dashed thick iso-line is the −10 m s^{-1} contour of DtC (no ENSO). In (a) and (b), the solid and dashed u-wind anomaly profiles are relative to DtC (strg ENSO) & DtC (no ENSO) respectively. Panel (c) and (d) the box plot show SSTAs spread across months in each basin. The latter include the sub-tropical north Atlantic (sub_NATL), the extra-tropical north hemispheric Atlantic (NH_NATL), the Mediterranean sea (MEDIT), the equatorial Atlantic (Eq_ATL), the South Atlantic (SH_ATL) and the Equatorial Eastern Indian ocean (Eq_IND).

These basin warmings and the regional-to-sub-regional atmospheric circulation features make the INT droughts not wide spread droughts like the DtC category but tend to be mixed dry and wet seasons i.e. hybrid rainy seasons.

Years since 1970s are believed to include anthropogenic climate change signature with the indirect GHGs forcing-induced SSTAs which caused past droughts in the Sahel [5]. With the increasing global warming, tropical oceans are also warming [9] and temperatures in most parts of the Sahel increased in the recent years [4, 5, 8, 10]. While most of the atmospheric large scale and sub-regional scale drivers of rainfall such as the Sahara Heat Low have become more enhanced [4, 21], recent climate model experiments suggest a direct influence of higher levels of

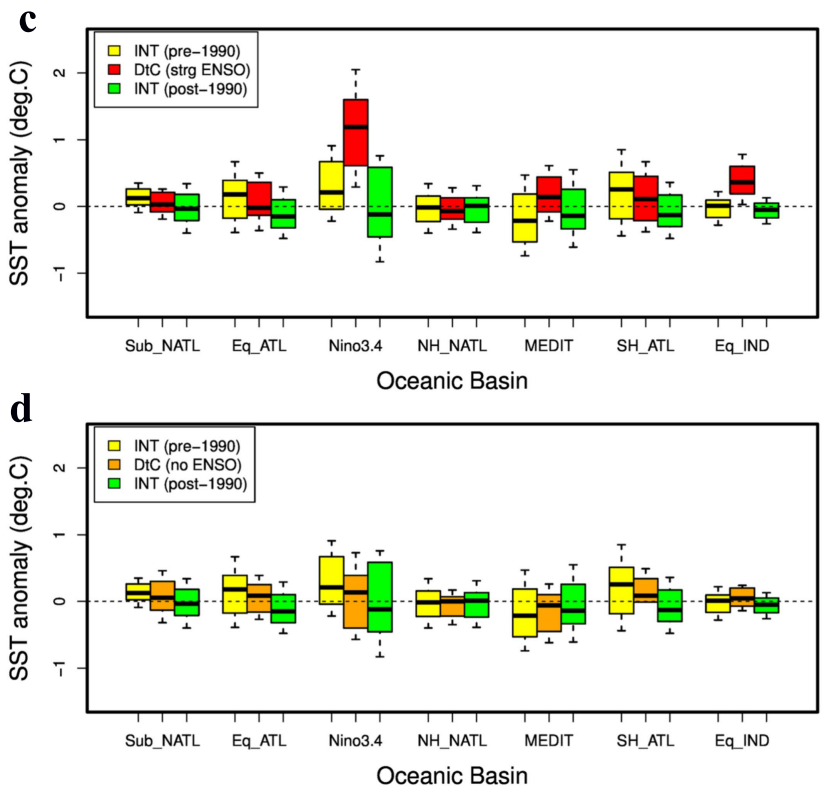

Figure 4. (Continued.)

GHGs in the atmosphere as the main cause of this recovery in rainfall amounts [10], with an additional role for surface air temperatures [4, 10, 21]. Although, these climate model results need further investigations to better established the direct influence of GHG on the long term climate of the Sahel [5, 28], the rapidly increasing air pollution might have also affected the regional climate [11]. Like the seasonal rainfall totals, MCS sizes, organization and intensity have also increased slightly after the mid-1980s [26]. The combination of the aforementioned factors with the upper wind patterns will most likely lead to increasing hybrid rainy seasons.

4. Discussion and recommendations

The recent partial recovery of annual rainfall amounts fluctuating around the long-term mean with an increase in extreme rainfall events, indicate an intensification of the hydrological cycle [5]. The local climate is drier in the sense of persistent dry spells compared to the 1950s–1960s [14], while at the same time there is an increased probability of floods [7, 8]. The statistical significance levels of this recovery, for the years after 1990 (including its features of high variability), have been demonstrated [2, 3, 5–7]. However, the process-based assessments needed to explain and hypothesize on plausible future trends are lacking [28]. The recent model-based arguments provided by Dong and Sutton [10], stating that green-house gases forcing has the most important role in this recovery, are to be taken with caution because of the internal errors inherent to single model results [5, 28]. In this paper, we bring forth additional process-based arguments provided by observations consensus and reanalysis data. The post-1990 recovery in the Sahel is dominated by hybrid rainy seasons explained by the combined effects of Ocean basins warming and the asymmetric regional low-to-mid-level atmospheric winds pattern. All atmospheric features displayed on figures 3 and 4 (and supplementary figures 5 and 6) have been rated statistically significant (only features significant at 95% confidence level according to a pulled-variance Student t-test were highlighted for surface pressure, wind, and SSTAs). Therefore, these results add value to hypotheses proven by previous other works concerning the importance of the internal variability of the regional climate [4, 9, 11, 21, 26, 28].

For a variety of agricultural practices, many risk factors are inherent to hybrid rainy seasons which are only observable from on-farm surveys and experiments. The erratic distribution of events leads to higher rates of re-planting, post-flowering water stress of up-land crops, flooding and water-logging of low-land cereals. The potential depletion of arable land and micronutrients due to water erosion is higher as a result of intense rainfall events. The increase in temperatures leads to heat stress, increased crop water demand, increased respiration rate, suppressed floral development, hastening crop maturity and reduce productivity [6]. The drought thresholds presented

here are useful for agroclimatic monitoring better than some areal drought metrics based on rainfall and other variables which tend to be relatively sensitive to certain mathematical formulations, the variables used to compute them, or the baseline period used to establish the reference climatology. If droughts were to occur [1, 29] or hybrid rainy seasons remain the dividends of the natural climate variability in this region, the profiling analysis of drought thresholds will improve the operational monitoring and early warning services for water management and farming systems. With the consistent relationship between seasonal droughts and DTR anomalies, the use of DTR will improve the monitoring of hybrid rainy seasons (i.e. DTR as a proxy variable beside rainfall amount and number of rainy days). Under global warming, we recommend the use seasons belonging to the DtC and their associated threshold values as the new standards for early detection of agroclimatic extremes to complement the existing areal monitoring indices.

In all Sahel countries, there is a limited availability of high quality, real-time *in situ* data because the density of local observation networks is mostly low [17, 30], some crucial atmospheric variables are less observed [11], and data collection and transmission are done manually with many outdated equipment. Our other recommendation is that longer term programs, supporting climate information services, should include infrastructural improvement of the hydro-climate observation networks but also the services *value chain* must include climate field schools and response farming [6, 31] to translate the seasonal rainfall variability into farming options that will spur smallholder farming system to build resilience. This will improve the quality of local climate information, its use by farmers and the availability of real-time *in situ* data, improve seamless predictions, and enable transboundary data sharing policies amongst countries so that global data centers can also improve their products for the region. We urgently advocate that the national adaptation programs of action, in countries of the Sahel, address hydro-climate observation networks and agroclimatic extension services.

Acknowledgments

This work was funded by the German Federal Ministry of Education and Research (BMBF) through the West African Science Center for Climate Change and Adapted Land Use (WASCAL). We thank all national meteorological services/agencies for contributing observed data. We acknowledge valuable comments from Patrick Laux on an earlier version of this document.

Author contributions

SS, CK, AG, JB and HK conceived and designed the research. SS, BS, JB, NB, and ONW contributed *in situ* data. ONW, NB and SS performed field experiments and crop model simulations. All authors worked together on the analysis and to write the manuscript.

Competing financial interest

The authors declare no competing financial interests.

References

[1] Trenberth K E, Dai A, van der Schrier G, Jones P D, Barichivich J, Briffa K R and Sheffield J 2014 Global warming and changes in drought *Nat. Clim. Change* **4** 17–22
[2] Lebel T and Ali A 2009 Recent trends in the Central and Western Sahel rainfall regime (1990–2007) *J. Hydrol.* **375** 52–64
[3] Maidment R I, Allan R P and Black E 2015 Recent observed and simulated changes in precipitation over Africa *Geophys. Res. Lett.* **42** 1–10
[4] Evan A T, Flamant C, Lavaysse C, Kocha C and Saci A 2015 Water vapour forced greenhouse warming over the Sahara desert and the recent recovery from the Sahelian drought *J. Clim.* **28** 108–23
[5] Giannini A 2015 Climate change comes to the Sahel *Nat. Clim. Change* **5** 720–1
[6] Salack S, Sarr B, Sangare S K, Ly M, Sanda I S and Kunstmann H 2015 Crop-climate ensemble scenarios to improve risk assessment and resilience in the semi-arid regions of West Africa *Clim. Res.* **65** 107–21
[7] Sanogo S, Fink A H, Omotosho J A, Ba A, Red R and Ermert V 2015 Spatio-temporal characteristics of the recent rainfall recovery in West Africa *Int. J. Climatol.* **35** 4589–605
[8] Ly M, Traore S B, Agali A and Sarr B 2013 Evolution of some observed climate extremes in the West African Sahel *Weather Clim. Extrem.* **1** 19–25
[9] Giannini A, Salack S, Lodoun T, Ali A, Gaye A T and Ndiaye O 2013 Unifying view of climate change in the Sahel linking intra-seasonal, interannual and longer time scales *Environ. Res. Lett.* **8** 024010
[10] Dong B and Sutton R 2015 Dominant role of greenhouse-gas forcing in the recovery of Sahel rainfall *Nat. Clim. Change* **5** 757–60
[11] Knippertz P, Evans M J, Field P R, Fink A H, Liousse C and Marsham J H 2015 The possible role of local air pollution in climate change in West Africa *Nat. Clim. Change* **5** 815–22
[12] Laux P, Kunstmann H and Bárdossy A 2008 Predicting the regional onset of the rainy season in West Africa *Int. J. Climatol.* **28** 329–42
[13] Sivakumar M V K 1992 Empirical analysis of dry-spells for agricultural applications in West Africa *J. Clim.* **5** 532–9
[14] Salack S, Giannini A, Diakhaté M, Gaye A T and Muller B 2014 Oceanic influence on the subseasonal to interannual timing and frequency of extreme dry spells over the West African Sahel *Clim. Dyn.* **42** 189–201
[15] http://ggweather.com/enso/oni.htm
[16] Belko N *et al* 2014 Selection for postflowering drought resistance in short- and medium- duration cowpeas using stress tolerance indices *Crop Sci.* **54** 1–9
[17] Lorenz C and Kunstmann H 2012 The hydrological cycle in three state-of-the-art reanalyses: Intercomparison and performance analysis *J. Hydrometeorol.* **13** 1397–420
[18] McKee T B, Doesken N J and Kleist J 1993 The relationship of drought frequency and duration to time scales *Eighth Conf. on Applied Climatology (Anaheim, CA) (American Meteorological Society)* pp 179–84
[19] Vicente-Serrano S M, Begueria S and Lopez-Moreno J I 2010 A Multi-scalar drought index sensitive to global warming: the standardized precipitation evapotranspiration index–SPEI *J. Clim.* **23** 1696–718
[20] Lyon B 2004 The strength of El-Niño and the spatial extent of tropical drought *Geophys. Res. Lett.* **31** L21204

[21] Giannini A 2010 Mechanisms of climate change in the semiarid African Sahel: the local view *J. Clim.* **23** 743–56
[22] Lélé I M, Leslie L M and Lamb P J 2015 Analysis of low-level atmospheric moisture transport associated with the West African Monsoon *J. Clim.* **28** 4414–30
[23] Ndiaye O, Ward N M and Thiaw W M 2011 Predictability of seasonal Sahel rainfall using GCMs and lead-time improvements through the use of a coupled model *J. Clim.* **24** 1931–49
[24] Chen T C and van Loon H 1987 Interannual variations of the tropical easterly jet *Mon. Weather Rev.* **115** 1739–59
[25] Nicholson S 2009 On the factors modulating the intensity of the tropical rainbelt over West Africa *Int. J. Climatol.* **29** 673–89
[26] Bell M A and Lamb P J 2006 Integration of weather system variability to multidecadal regional climate change: the West African Sudan-Sahel Zone, 1951–98 *J. Clim.* **19** 5343–65
[27] Gaetani M and Fontaine B 2013 Interaction between the West African Monsoon and the summer Mediterranean climate: an overview *Fís. Tierra* **25** 41–55
[28] Janicot S *et al* 2015 The recent partial recovery in sahel rainfall: a fingerprint of greenhouse gases forcing? *GEWEX News* **27** 11–4
[29] Dai A 2013 Increasing drought under global warming in observations and models *Nat. Clim. Change* **3** 52–8
[30] Jones L *et al* 2015 Ensuring climate information guides long-term development *Nat. Clim. Change* **5** 812–4
[31] Stigter K, Winarto Y T, Ofori E, Zuma-Netshiukhwi G, Nanja D and Walker S 2013 Extension agrometeorology as the answer to stakeholder realities: response farming and the consequences of climate change *Atmosphere* **4** 237–53
[32] Hoogenboom G *et al* 2015 *Decision Support System for Agrotechnology Transfer (DSSAT) Version 4.6* (Prosser, WA: DSSAT Foundation) (http://dssat.net)